Condition Monitoring of roller bearings using Acoustic Emission

Daniel Cornel[1], Francisco Gutiérrez Guzmán[1], Georg Jacobs[1], Stephan Neumann[1]

[1]Chair for Wind Power Drives (CWD), RWTH Aachen University, Aachen, 52074, Germany

Correspondence to: Daniel Cornel (daniel.cornel@cwd.rwth-aachen.de)

Abstract. Roller bearing failures in wind turbines gearboxes lead to long downtimes and high repairing costs, which could be reduced by the implementation of a predictive maintenance strategy. In this paper and within this context an acoustic emission based condition monitoring system is applied to roller bearing test rigs with the aim of identifying critical operating conditions before bearing failures occurs. Furthermore, a comparison regarding detection times is carried out with a traditional vibration based condition monitoring systems, with focus on premature bearing failures such as white etching cracks. The investigations show a sensitivity of the acoustic emission system towards lubricating conditions. In addition, the system has shown, that a damaged surface can be detected at least ~4 % (8 hours, regarding the time to failure) earlier than by using the vibration based system. Furthermore, significant deviations from the average acoustic emission signal were detected up to ~50 % (130 hours) before the test stop and are possibly related to sub-surface damage initiation and might result in an earlier damage detection in the future.

1 Introduction

A large part of downtimes and repairing costs of wind turbines (WT) are caused by gearbox roller bearing failures (Sheng, 2015). The most cost-effective solution to these standstills is to prevent catastrophic failure involving on the one hand the premature detection of damage pre-stages and on the other hand the identification of critical operating conditions and adapting the operating strategy accordingly. Typically, condition monitoring systems (CMS) in wind turbines monitor vibration, temperatures and oil contamination (Tchakoua et al., 2014). These parameters are very well suited to detect any macroscopic damages of individual components such as gearbox bearings. The classical CMS are, however, not applicable for the detection of damage pre-stages, like crack initiation or propagation, nor for the identification of critical operating conditions, such as low lubrication regimes or excessive sliding. For this purpose, the use of Acoustic Emission (AE) could be a suitable solution. This technology has already proven itself for the crack detection on pressure tanks (DGZfP, 2011) and its applicability for the monitoring of rotating components is being researched with promising results. Nonetheless, there are still several challenges to be addressed such as ambient noises or the differentiation between individual, overlapping signals of individual components such as bearings, gears and couplings (Elasha et al., 2017). Therefore, to exploit AE's capabilities at component or system level, it is necessary to gain further experience regarding operating conditions and system behaviour for certain events like surface damages.

30 Within this context, investigations were carried out in this study at component level using both a downscaled radial and thrust bearing test rig with installed AE sensors. The current work is separated into two parts. The first part addresses the analysation of the AE system sensitivities towards operating conditions causing roller bearing failures. Within the second part it is intended to give a statement regarding damage detection times using AE and typical WT vibration sensor in order to assess the potential of AE for premature detection of bearing damages. In addition, it is discussed if the development of a sub-surface initiated

35 rolling bearings damage can be detected by the AE system. It should also be mentioned that the first part refers to a test series which has already been published (Cornel et al., 2018). Within the framework of this work, a slightly more detailed examination of possible causes for the former presented AE system behaviour and, in addition, an assignment of the results towards typical roller bearing failure mechanisms are carried out. The second part is based on unpublished research (statement regarding damage detection times).

40 **2 State of the art**

The use of AE-CMS is the subject of current research. A differentiation of published research can be carried out using the used test level used by the corresponding authors:

- Model level e.g. on tensile/compression/four-point bending specimens or disc tribometers

- Component level e.g. on roller bearings, plain bearings or gear wheels

45 - Subsystem or system level, e.g. using gears or wind turbines.

In contrast to component and system levels, investigations at the model level offer the advantage that useful or interfering signals can be better identified. For this reason, these investigations provide a first contribution to the analysis of the AE signals regarding the identification, characterization and classification of signals at component and system level. For example, by using tensile and compression tests at the model level it was found that the occurrence of AE signals correlates more with the

50 applied stress intensity than with the crack growth rate and is thus more related to the plastic volume at the crack tip (Morton et al., 1973). In further investigations, AE signal properties, e.g. counts (Roberts and Talebzadeh, 2003; Bruzelius and Mba, 2004; Singh et al., 2007), could be correlated with crack growth and thus with the state of the tensile specimen.

In addition to demonstrating the applicability of AE-CMS for the detection of damage pre-stages, current research on the component level focuses on the use of AE-CMS to evaluate the prevailing operating conditions. Particularly in the field of

55 rolling bearing technology, a large number of investigations are concerned with the comparison of AE signals of undamaged and artificially damaged bearing components, followed by the assignment to the extent of damage. AE-CMS peak values, kurtosis and RMS of the AE signals often allow the aforementioned distinctions (Shiroishi et al., 1997; Choudhury and Tandon, 2000; Morhain and Mba, 2003; Al-Ghamd and Mba, 2006). With regard to the analysis of the operating condition, AE-CMS has so far shown that, for example, the AE RMS or energy values are related to speed and load levels and thus to the lubrication

60 condition (expressed by the specific lubricating film height), but partly with conflicting results regarding the interactions (Cockerill et al., 2016; Cornel et al., 2018; Couturier and Mba, 2008; Morhain and Mba, 2003; Ferrando Chacon et al., 2015).

2003 - 2007
STATE OF THE ART?

Investigations between the AE signals and the degree of lubricant contamination on rolling bearings have shown that it is possible to distinguish between contaminated and clean lubricants (Schnabel et al., 2017; Miettinen and Andersson, 2000). Furthermore, the monitoring of service life tests of rolling bearings shows an increase of the AE signals towards the end of the

65   service life and, in comparison with the classical vibration based CMS, provides significantly earlier indications of damage (Eftekharnejad et al., 2011; Barteldes et al., 2014). While shaft speeds of at least 300 rpm were frequently used in the aforementioned investigations, the monitoring of slow-running rolling bearings with shaft speeds <300 rpm is in focus of current research. For example, the observations regarding the increase in AE signals towards the end of the service life and the higher sensitivity to vibration based CMS have already been confirmed at rotating speeds of <100 rpm (Elforjani, 2018) and

70   <60 rpm (van Hecke et al., 2016). For further information regarding this speed range, the summary in (Caesarendra et al., 2016) is recommended.

Compared to the AE investigations on rolling bearings, the results related with plain bearings are significantly more advanced regarding the usability of the signals. This may be due to the lower number of contacts and components. In plain bearing applications, for example, it is possible to map the Stribeck curve using AE RMS or AE energy values and thus to identify the

75   prevailing lubrication condition compared to investigations on rolling bearings (Mirhadizadeh et al., 2010; Mokhtari et al., 2017; Fritz et al., 2001). These results were confirmed in (Mokhtari et al., 2018) and furthermore it was found that the kurtosis values of the AE signals and the consideration of the mean frequencies can be used for a distinction between mixed friction and full lubrication regimes. In addition, a regular comparison of the Stribeck curves generated by AE RMS values allows a statement regarding the progress of wear and the remaining service life (Mokhtari et al., 2018). Recent studies, e.g. by

80   PODDAR et. al (Poddar and Tandon, 2019) show that the AE RMS and AE energy values in plain bearings can also be correlated with the degree of contamination of the oil and the particle size of the contamination.

In addition to the mentioned applications in the rolling and plain bearing area, other areas are also considered in the literature. For example, the monitoring of gears regarding tooth damage (Scheer et al., 2007), the monitoring of cutting processes with regard to cutting forces, surface quality and tool condition (Venkata Rao and Murthy, 2018; Filippov et al., 2017; Ferrari and

85   Gómez, 2015) and the monitoring of shafts with regard to alignment, crack initiation and crack propagation (Ferrando Chacon et al., 2014; Elforjani and Mba, 2009, 2009, 2011).

In summary, the results show that the evaluation of AE signals enables both the detection of component damage and an evaluation of the present operating condition. With a change from model level to component level, however, the number of interfering signals increases, so that further research is required in the field of signal processing and signal assignment.

90   Regarding the analysis of subsystem or system levels, the work in connection with AE often focuses on (planetary) gears with the aim of localizing the signal origin and correlating it with the degree of damage of the affected component. Using a 2 kW spur gear it could be shown, for instance, that the degradation of the gear could be correlated by means of AE RMS values and offers a significantly better signal-to-noise ratio compared to vibration sensors (Qu et al., 2014). In planetary gears on a laboratory scale, a relative error of 5 teeth on average was achieved in the localization of damage during operation using 4 AE

95   sensors (Zhang et al., 2017). When considering power classes that are more relevant for wind turbines, it was possible to locate

the AE source with an accuracy of up to 2 teeth at stationary 850 kW and 1.5 MW planetary gears using at least 3 AE sensors (Leaman et al., 2019).

This brief overview shows that AE CMS is a subject of research in a variety of areas and thus of general interest. Focussing on rolling bearing applications, it could be stated that there is a lot of work related to the detection of artificial damages, without

100 monitoring the overall damage development. In this context, AE CMS appears to be more sensitive to the detection of artificial damage than vibration based CMS. The research on monitoring the operating conditions shows that AE CMS offers further possibilities than other CMS. However, it appears that these sensitivities are achieved on single bearing test rigs or disc tribometers and therefore are often system-specific with limited transferability.

Within the scope of this work, the analysation of the AE system sensitivities towards operating conditions causing roller

105 bearing failures, the assessment of AE regarding the potential for premature detection of bearing damages and the application of AE on multi-bearing test rigs shall contribute to the state of the art.

3 Test benches and Acoustic Emission sensors

Four-bearing test bench: The investigations regarding the detection of operating conditions were conducted on a four-bearing test bench (Figure 1). This test rig consists mainly of a drive unit, a radial load unit, an oil chamber and four test bearings from

110 type NU206-TVP2 with a bore diameter of 30 mm. The radial load unit consists of a disc spring stack, which can be statically pre-loaded. The radial load is applied through the two middle test bearings. The test bearings are mounted on a shaft, which is driven by an electric motor (max. 6,000 rpm). The loaded shaft itself is mounted in the test head by the outer test bearings, which are each arranged symmetrically to each other ensuring a symmetrical load distribution on the test bearings.
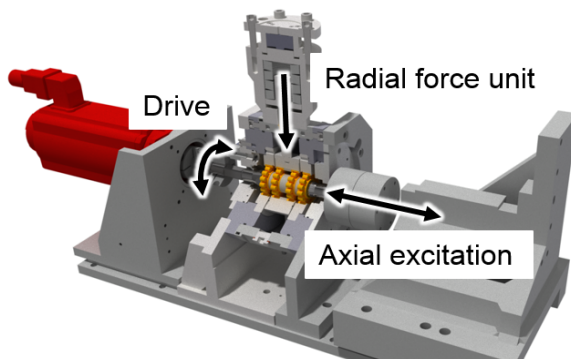
Test bench	RLP
Shaft diameter [mm]	30
No. of test bearings [-]	4
Bearing type	NU206
Radial load [kN]	100
Axial load [kN]	8/100 (high frequency/static)
$p_{Hertz, max}$ [MPa]	3,600
Test temperature [°C]	40-110

115 **Figure 1: Four-bearing test bench (RLP), shaft diameter 30 mm.**

Thrust bearing test bench: The fatigue related tests in this work were carried out using cylindrical roller thrust bearings of type 81212 in an FE8 type test rig (Deutsches Institut für Normung e. V., 2016), see Figure 2. The standard FE8 uses a constant load spring system, designed for bearing loads up to 100 kN. Using an electrical drive, it is possible to set-up a shaft speed between 7.5-300 rpm. In case of exceeding a limit bearing temperature or vibration level (e.g. caused by a pitting) the test will

120 be stopped automatically. Two test bearings are used for each test run. These are often distinguished on the basis of their

position within the test rig. Thus, there is a bearing at the motor-side and a bearing at the housing side of the test rig. Each bearing consists of two washers, a cage and the rolling elements. One washer is mounted on the shaft and is driven, while the other one is stationary placed in the housing.

Test bench	FE8
Shaft diameter [mm]	60
No. of test bearings [-]	2
Bearing type	81212
Radial load [kN]	0
Axial load [kN]	60
p_{Hertz} [MPa]	1,790
Test temperature [°C]	100
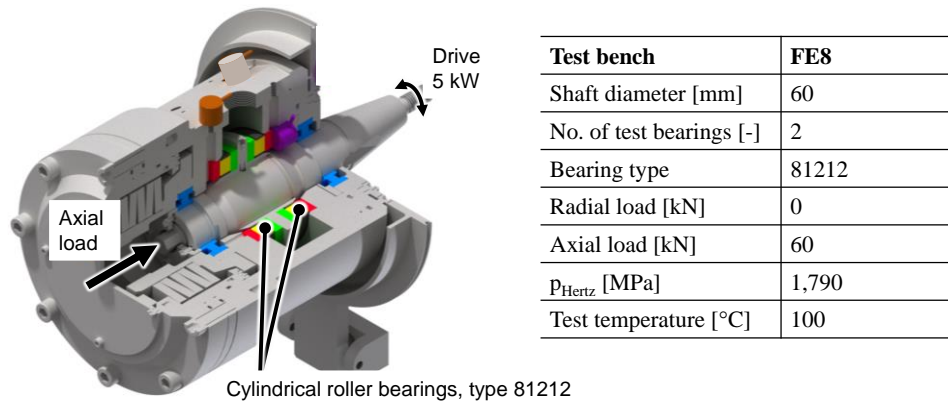
125 **Figure 2: FE8 type test rig with test bearings of type 81212 according to (Deutsches Institut für Normung e. V, 2016).**

Acoustic Emission sensors: Beside classic vibration sensors, Acoustic Emission sensors were used. The sensors are broadband sensors (Model: QWT-MCX) of the company QASS and shown in Figure 3. Unfortunately, no frequency response diagram of the sensor was available at the time of publication.
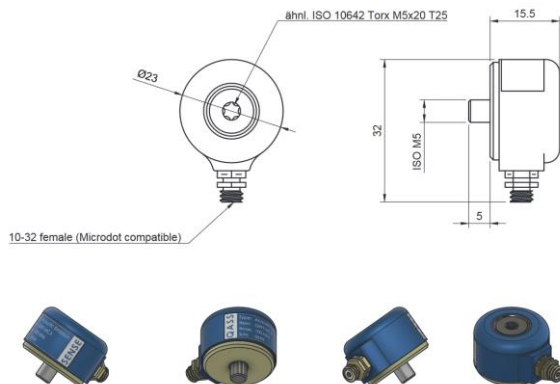
130 **Figure 3: Used Acoustic Emission sensors.**

Although both methods rely on the same operating principle, the Acoustic Emission (AE) sensors have no seismic mass. As a result, AE sensors can be used in higher frequency bands (Cockerill, 2017), often with range of 100 kHz to 1,000 kHz. On the other hand, vibration sensors operate in a band between 0 and 50 kHz. Therefore, AE operates outside the frequency range of classic machine vibrations and is less sensitive towards typical background noises such as test bench cooling system (PAC,
135 2015). Nevertheless, our own research has shown that a variety of high frequencies cause noise that reduces the signal-to-noise ratio. To increase the accuracy, the sensors need to be installed as close as possible to the rolling contacts.

In the case of the four-bearing test bench, 4 sensors were installed. For the middle test bearings (# 2 & 3) the sensors can be easily installed within the test head, shown in Figure 4. In the case of the outer test bearings (# 1 & 4) the sensors need to be installed outside the housing due to lack of space.

140
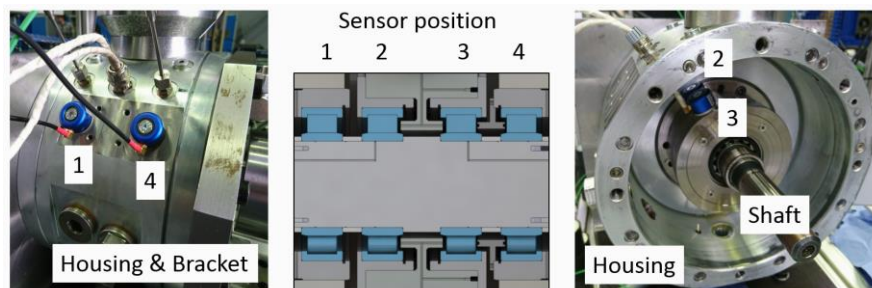
Figure 4: Four-bearing test bench (RLP): position of the installed AE sensors.

For use on the thrust bearing test rig, the sensors had to be installed outside the housing again due to the lack of space. The actual installation position of the sensors is shown in Figure 5. While the vibration sensor is preferably placed in the direction of excitation, our own preliminary investigations show that AE sensors mounted in the displayed position provide the best

145   results due to the short distance to the roller bearings. A positioning in direct proximity to the vibration sensor would be technical possible, but results in a significant increase in the required component crossings and the distance to the bearings in general and thus in a change and lowering of the AE signals.
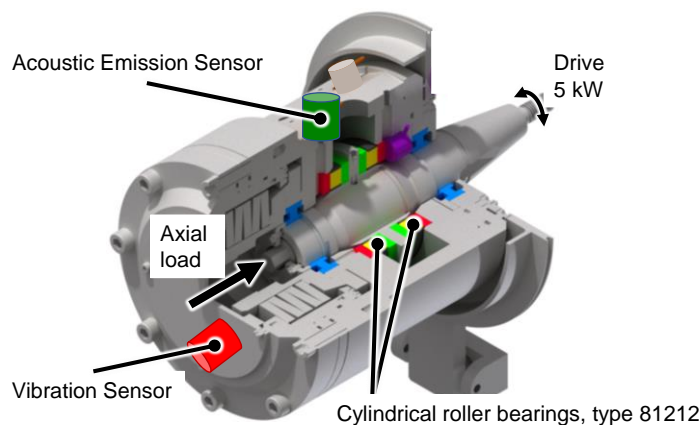
Figure 5: Thrust bearing test bench: position of the AE and vibration sensor.

150   **4 Experimental method and Results**

The aim of this work is to investigate sensitivities of the AE system towards operating conditions causing roller bearing failures on one hand and on the other hand to investigate the differences regarding the detection time of AE and typical WT vibration sensor in order to assess the potential of AE for premature detection of bearing damages. In addition, it is discussed if the development of a sub-surface initiated rolling bearings damage can be detected by the AE system

155

AE sensitivities towards the detection of operating conditions

Typical failure modes of roller bearings in wind turbine gearboxes are Micro-pitting, Smearing (Scuffing, Rehardening), and White Etching Cracks, as shown in (Sheng, 2015). A short explanation of these failure modes can be found in previous work (Cornel et al., 2018). In addition, the following literature is recommended for a more detailed insight (Bongardt, 2015; van

160 Lier, 2015; Gutiérrez Guzmán et al., 2018; Gutiérrez Guzmán et al., 2020).

Generally speaking, the operating conditions of a bearing are depending on the load (F), the shaft speed (n), the resulting bearing temperature (T), the lubricant and the roughness of bearing components. In this work a lubricant ISO VG 100 was used. Furthermore, it was ensured that the roughness of the used bearings was between 0.03 and 0.08 µm. The aforementioned factors are used to calculate the specific lubricant film thickness lambda "λ", which is used as a quantitative indicator of the

165 lubricating conditions prevailing in the contact area. Values of $\lambda \geq 3$ indicate full fluid lubrication conditions, values of $\lambda \leq 1$ indicate boundary lubrication conditions while the range between is referred to as mixed lubrication regime (Czichos and Habig, 2015). An operation under full fluid lubrication is intended in general. For the calculation of lubricant film thickness, the reader is referred to the work of DOWSON and HIGGINSON (Dowson and Higginson, 1966). In the following Figure 6, the main influencing parameters are briefly highlighted.
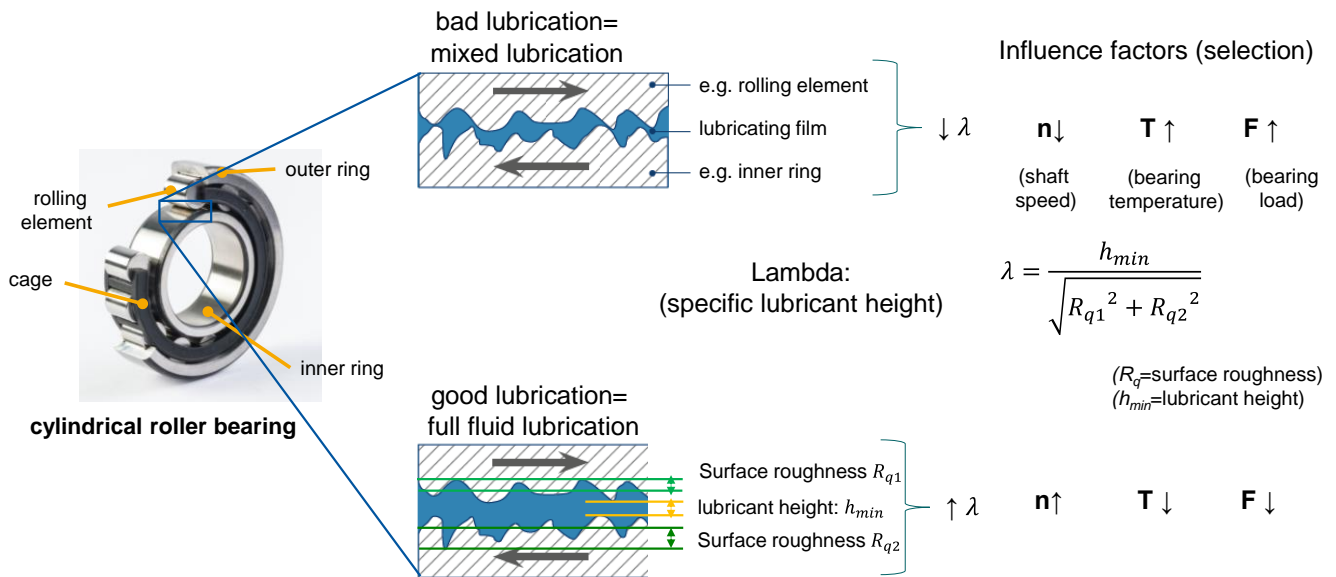
170

Figure 6: Brief explanation of the lubrication state and the influence factors.

It should be noted that the possible influence of static/dynamic load levels, slide-roll-ratio, stillstand, current passage, are consciously neglected in this work.

The above-mentioned failure modes (Micro-pitting, Smearing, White Etching Cracks) are among other things promoted by

175 boundary and mixed lubrication conditions. Under full fluid lubrication conditions, the surfaces are completely separated, and the maximum stress shifts further below the surface, which is a prerequisite for typical rolling contact fatigue damage. Using

the influencing factors on the specific film thickness such as e.g. shaft speed, temperature and load, and specific lubricating conditions can be set on a test bench.

The following experiment regarding the Influence of the lubrication regime was part of a test series presented in previous work
180 (Cornel, 2018). Due to the strong dependence of the specific lubricant film thickness on the oil temperature was used to adjust different lubrication conditions. To expand the parameter field two different shaft speeds, 500 and 3,000 rpm, were used. The investigations were carried out at a constant pressure of 2.0 GPa while the temperature itself was varied between 30 and 130 °C. Figure 7 shows the results of the experiments.
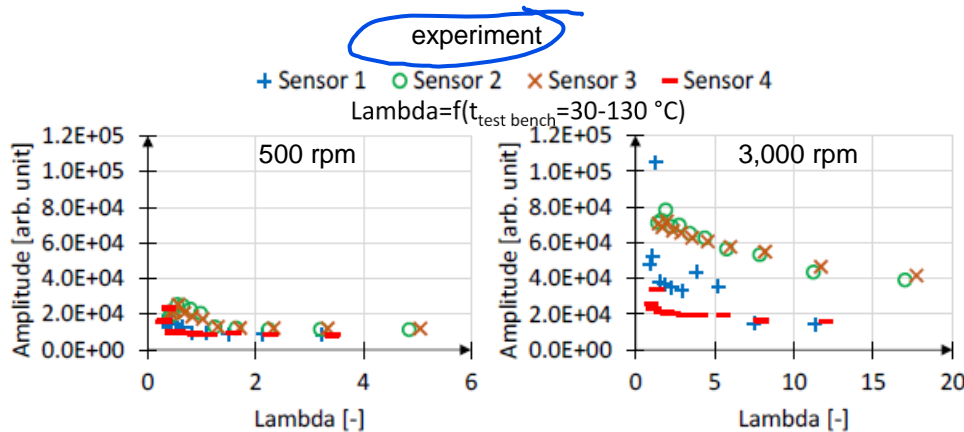
185 **Figure 7: Influence of the lubrication regime and the shaft speed on the AE Energy level.**

It can be observed that the amplitude of the AE signals increases as lambda decreases. This is especially noticeable in the areas around λ =0.5-2. At 500 rpm (Figure 7 – Left) and λ > 2 the amplitude remains almost constant. The results meet the expectations that an increasing separation of the surfaces, defined by an increasing lambda, leads to decreased acoustic signals due to the missing interaction of roughness spikes within the contact. On the other hand, at 3,000 rpm (Figure 7- right) the

190 effect the AE amplitude remaining constant can only be seen by the external sensors, 1 and 4, at λ-values > 5. Sensor 2 and 3 still show a significant decrease of the amplitude with an increasing lambda. This could be explained as follows: The transfer path of the acoustic signals to the externally mounted sensors has two additional component transitions due to the test rigs design and is about 350 % longer compared to the internally mounted sensors. This consideration can lead to the fact that the signals become weaker and may no longer be detected. Regarding the significant decrease of the amplitude with an increasing

195 lambda at 3,000 rpm, it is assumed that due to the significantly higher shaft speed, the whole system is excited (e.g. the vibration of test rig itself, increase of the bearing over rolling frequencies) much more and therefore resulting in an higher amplitude of the signals. Figure 8 arranges the results with the conducive conditions of the aforementioned failure modes. In conclusion it can be said, that for a known system or test bench the magnitude of the AE amplitude can be used to roughly determine the rotation speed range of the system.
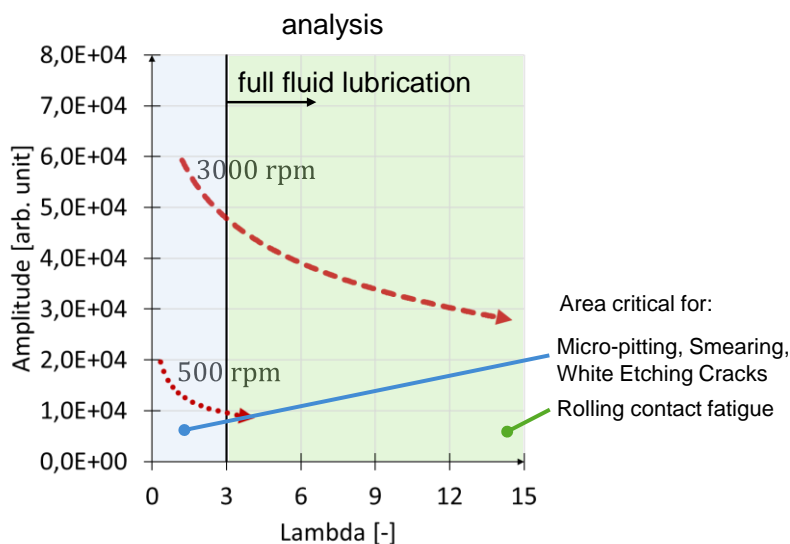
Figure 8: AE results arranged with the lubrication regimes.

In addition, it is possible to distinguish between mixed friction and full fluid lubrication for the corresponding speed level. Therefore it can be concluded, that a first analysis of the criticality of the prevailing conditions accompanied by an estimation of the expected failure mechanism could be carried out by using a CMS based on AE as long as the system is known from previous investigations or a measurement phase is implemented during the set up process.

Development of a roller bearing damage

In order to compare the time to failure detection of CMS´s based on AE and vibration under known conditions the thrust bearing test rig ("FE8") introduced in chapter 3, was used. This test rig was chosen because it allows to generate a bearing within a short period of time. Due to the recent relevance, conditions were chosen which additionally lead to a WEC damage. A WEC-induced bearing failure can occur after 5-20% of the L_{10} nominal lifetime (Evans, 2015) and is therefore considered particularly critical. Further information can be found in the work of DANIELSEN et al. (Danielsen et al., 2017). The testing was carried out within a short period of time (< 500 h) using well known operating conditions. The test conditions are characterised by an axial load of 60 kN, a shaft speed of 300 rpm and a bearing temperature of 100 °C. These conditions have been previously used in further FE8 related WEC studies such as (Danielsen et al., 2019). As shown in the work of DANIELSEN (Danielsen et al., 2019) these conditions usually lead to failures between 100 h and 300 h.

During testing and as aforementioned, the signal of a vibration sensor and an AE sensor were monitored continuously during testing. Figure 9 shows both averaged signals form one test over the total test time of ~261 h. The signal of the vibration sensor, shown as a red line, is plotted as root mean square (RMS) and therefore marked as RMS. In contrast the AE signal, plotted as green line, shows the amplitude average and is marked as AE average. The test was stopped after 261 h due to the vibration

signal exceeding the vibration threshold (20 % above the RMS value after run-in). Post-testing analysis confirmed a pitting damage as the source for the increased vibration.
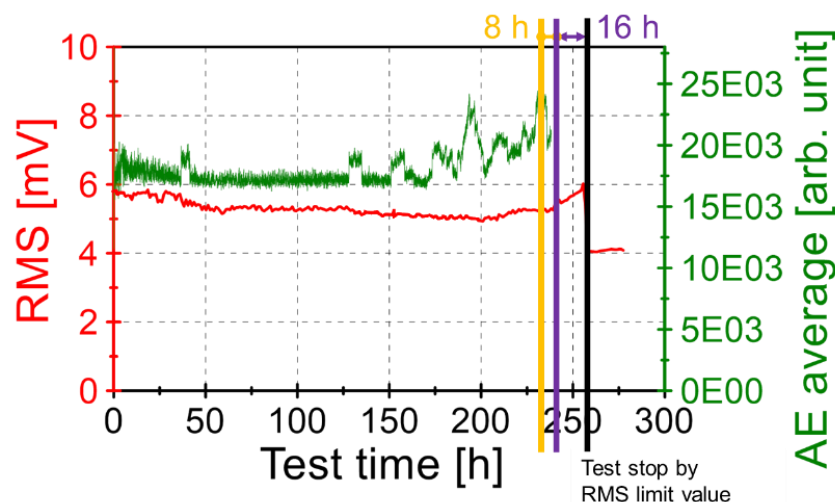
Figure 9: Comparison of vibration and AE signal over the test time.

225 Regarding the signal behaviour, both show a decreasing tendency within the first 50 h. This tendency can be correlated with typical running-in processes (e.g. smoothing of the roughness peaks on the bearing surface). Subsequently, the vibration signal stays at an almost constant level before it rises significantly approx. 16 h before the threshold is exceeded. In contrast, the averaged AE signal shows the first indications of a deviation from its constant level after a test time of 125 h. These deviations increase significantly from about 150 h and 175 h onwards. Unfortunately, it should be noted that the last 16 hours of the AE

230 signal are missing due to a recording error. In comparison with the vibration sensor, it can be concluded that significant activities of the AE system are visible at least 8 h before the vibration signal rises (referred to the latest peak of the AE signal before the test stop). It is assumed, that the latest AE signal activities together with the increased AE signal level in general can be traced back to the formation of the pitting or to the outbreak of the surface. The preceding activities are possibly caused by sub-surface damage initiation and propagation. These deviations were detected up to ~50 % (130 hours) before the test stop

235 and are potentially related to sub-surface damage initiation and might result in an earlier damage detection in the future. In general, AE signals can be associated, on a model level (see chapter 2), to damage pre-stages, such as crack initiation, crack-propagation or structural changes inside the bearing components. As described in chapter 2, the correlation of the AE signals to specific phenomena is however still a research subject. As a basis for the future investigation of the topic, the signals should be examined for characteristic attributes and validated in further experiments.

4 Summary & Outlook

In the conducted work two key aspects were covered. On the one hand, to analyse the sensitivities of the Acoustic Emission (AE) system towards operating conditions causing failures at radial roller bearings. And on the other hand, to give a statement regarding pre warning times for upcoming damages using AE and typical WT vibration sensors. In addition, it is discussed if the development of a sub-surface initiated rolling bearings damage can be detected by the AE system

The investigations on the radial bearing test bench have shown that the magnitude of the AE amplitude can be used to roughly determine the rotation speed range of a known system. In addition, it is possible to distinguish between an operation under mixed friction and full fluid lubrication regime for the corresponding rotation speed. Therefore, this study offers a first analysis of the theoretical criticality of the prevailing conditions accompanied by an estimation of the expected failure mechanism.

The investigations regarding the damage detection using a thrust bearing test rig (FE8) have shown that a pitting damage could be detected by the AE system at least ~4 % (8 hours) in advance of the vibration based system. Furthermore, noticeable deviations in the AE signal were detected up to ~50 % (130 hours) before the test stop and are possibly associated with damage pre-stages, such as crack initiation, crack-propagation or structural changes inside the bearing components and might result in an earlier damage detection in future. Besides, it was found that the AE system and the vibration based system are capable to detect the run-in period of a test run.

In the next step, the results are going to be validated on WT-size bearings. For this purpose a new four bearing test bench, with a shaft diameter of 180 mm will be used. Furthermore, it will be attempted to analyse the signals on a more detailed level, trying to get further and more general information.

Acknowledgements

The authors would like to thank the European Union and the German federal state of North-Rhine Westphalia (NRW) for the financial funding. They would also like to thank the Leitmarktagentur.NRW for the academic and administrative project support and all industrial partners for the good teamwork.

References

Al-Ghamd, A. M. and Mba, D.: A comparative experimental study on the use of acoustic emission and vibration analysis for bearing defect identification and estimation of defect size, Mechanical Systems and Signal Processing, 20, 1537–1571, https://doi.org/10.1016/j.ymssp.2004.10.013, 2006.

Barteldes, S., Walther, F., and Holweger, W.: Wälzlagerdiagnose und Detektion von WEC mit Barkhausen-Rauschen und Hochfrequenz-Impuls-Messung, 2014.

Bongardt, C.: Wälzlagergraufleckigkeit, Dissertation, Verlagsgruppe Mainz GmbH, Aachen, 2015.

270 Bruzelius, K. and Mba, D.: An initial investigation on the potential applicability of Acoustic Emission to rail track fault detection, NDT & E International, 37, 507–516, https://doi.org/10.1016/j.ndteint.2004.02.001, 2004.

Caesarendra, W., Kosasih, B., Tieu, A. K., Zhu, H., Moodie, C. A.S., and Zhu, Q.: Acoustic emission-based condition monitoring methods: Review and application for low speed slew bearing, Mechanical Systems and Signal Processing, 72-73, 134–159, https://doi.org/10.1016/j.ymssp.2015.10.020, 2016.

275 Choudhury, A. and Tandon, N.: Application of acoustic emission technique for the detection of defects in rolling element bearings, Tribology International, 33, 39–45, https://doi.org/10.1016/S0301-679X(00)00012-8, 2000.

Cockerill, A., Clarke, A., Pullin, R., Bradshaw, T., Cole, P., and Holford, K. M.: Determination of rolling element bearing condition via acoustic emission, Proceedings of the Institution of Mechanical Engineers, Part J: Journal of Engineering Tribology, 230, 1377–1388, https://doi.org/10.1177/1350650116638612, 2016.

280 Cockerill, A.: Damage Detection of Rotating Machinery, Thesis (PhD), Mechanics, Materials and Advanced Manufacturing Engineering, Cardiff University, Cardiff, 312 pp., 2017.

Cornel, D., Gutiérrez Guzmán, F., Jacobs, G., and Neumann, S. (Eds.): Acoustic response of roller bearings under critical operating conditions, 13 th World Congress on Engineering Asset Management, Stavanger, Norway, 10 pp., 2018.

Couturier, J. and Mba, D.: Operational Bearing Parameters and Acoustic Emission Generation, J. Vib. Acoust., 130, 24502,
285 https://doi.org/10.1115/1.2776339, 2008.

Czichos, H. and Habig, K.-H.: Tribologie-Handbuch: Tribometrie, Tribomaterialien, Tribotechnik, Springer Fachmedien Wiesbaden, Wiesbaden, 794 pp., 2015.

Danielsen, H. K., Gutiérrez Guzmán, F., Muskulus, M., Rasmussen, B. H., Shirani, M., Cornel, D., Sauvage, P., Wu, J., Petrov, R., and Jacobs, G.: FE8 type laboratory testing of white etching crack (WEC) bearing failure mode in 100Cr6,
290 Wear, 434-435, 202962, https://doi.org/10.1016/j.wear.2019.202962, 2019.

Danielsen, H. K., Gutiérrez Guzmán, F., Dahl, K. V., Li, Y. J., Wu, J., Jacobs, G., Burghardt, G., Fæster, S., Alimadadi, H., Goto, S., Raabe, D., and Petrov, R.: Multiscale characterization of White Etching Cracks (WEC) in a 100Cr6 bearing from a thrust bearing test rig, Wear, 370-371, 73–82, https://doi.org/10.1016/j.wear.2016.11.016, 2017.

Deutsches Institut für Normung e. V.: Testing of lubricants – Mechanical-dynamic testing in the roller bearing test apparatus
295 FE8: Part 1: General working principles, Beuth Verlag GmbH, Berlin, 11 pp., 2016.

DGZfP: Kompendium Schallemissionsprüfung Acoustic Emission Testing (AT): Grundlagen, Verfahren und praktische Anwendung, 2011.

Dowson, D. and Higginson, G. R.: Elastohydrodynamic lubrication: The Fundamentals of Roller and Gear Lubrication, Pergamon P, London, 124 pp., 1966.

300 Eftekharnejad, B., Carrasco, M. R., Charnley, B., and Mba, D.: The application of spectral kurtosis on Acoustic Emission and vibrations from a defective bearing, Mechanical Systems and Signal Processing, 25, 266–284, https://doi.org/10.1016/j.ymssp.2010.06.010, 2011.

Elasha, F., Greaves, M., Mba, D., and Fang, D.: A comparative study of the effectiveness of vibration and acoustic emission in diagnosing a defective bearing in a planetry gearbox, Applied Acoustics, 115, 181–195,
305 https://doi.org/10.1016/j.apacoust.2016.07.026, 2017.

Elforjani, M.: Diagnosis and prognosis of slow speed bearing behavior under grease starvation condition, Structural Health Monitoring, 17, 532–548, https://doi.org/10.1177/1475921717704620, 2018.

Elforjani, M. and Mba, D.: Condition Monitoring of Slow-Speed Shafts and Bearings with Acoustic Emission, Strain, 47, 350–363, 2011.

310 Elforjani, M. and Mba, D.: Detecting natural crack initiation and growth in slow speed shafts with the Acoustic Emission technology, Engineering Failure Analysis, 16, 2121–2129, https://doi.org/10.1016/j.engfailanal.2009.02.005, 2009.

Evans, M.-H.: An updated review: White etching cracks (WECs) and axial cracks in wind turbine gearbox bearings, Materials Science and Technology, 1–37, https://doi.org/10.1080/02670836.2015.1133022, 2015.

Ferrando Chacon, J. L., Kappatos, V., Balachandran, W., and Gan, T.-H.: A novel approach for incipient defect detection in
315 rolling bearings using acoustic emission technique, Applied Acoustics, 89, 88–100, https://doi.org/10.1016/j.apacoust.2014.09.002, 2015.

Ferrando Chacon, J. L., Artigao Andicoberry, E., Kappatos, V., Asfis, G., Gan, T.-H., and Balachandran, W.: Shaft angular misalignment detection using acoustic emission, Applied Acoustics, 85, 12–22, https://doi.org/10.1016/j.apacoust.2014.03.018, 2014.

320 Ferrari, G. and Gómez, M. P.: Correlation Between Acoustic Emission, Thrust and Tool Wear in Drilling, Procedia Materials Science, 8, 693–701, https://doi.org/10.1016/j.mspro.2015.04.126, 2015.

Filippov, A. V., Rubtsov, V. E., and Tarasov, S.Y.: Acoustic emission study of surface deterioration in tribocontacting, Applied Acoustics, 117, 106–112, https://doi.org/10.1016/j.apacoust.2016.11.007, 2017.

Fritz, M., Burger, W., and Albers, A.: Schadensfrüherkennung an geschmierten Gleitkontakten mittels
325 Schallemissionsanalyse, 2001.

Gutiérrez Guzmán, F., Sous, C., van Lier, H., and Jacobs, G.: An energetic approach for the prognosis of thermally induced white etching layers in bearing steel 100CrMn6, Tribology International, 143, 106096, https://doi.org/10.1016/j.triboint.2019.106096, 2020.

Gutiérrez Guzmán, F., Özel, M., Jacobs, G., Burghardt, G., Broeckmann, C., and Janitzky, T.: Influence of Slip and
330 Lubrication Regime on the Formation of White Etching Cracks on a Two-Disc Test Rig, Lubricants, 6, 8, https://doi.org/10.3390/lubricants6010008, 2018.

Gutiérrez Guzmán, F., Özel, M., and Pinard, P.: Risse auf Lagerringen - 707 II: Forschungsvereinigung Antriebstechnik, FVA, 2017.

Leaman, F., Hinderer, S., Baltes, R., Clausen, E., Rieckhoff, B., Schelenz, R., and Jacobs, G.: Acoustic Emission Source

335   Localization in Ring Gears from Wind Turbine Planetary Gearboxes, Forsch Ingenieurwes, 13, 1,

https://doi.org/10.1007/s10010-018-00296-4, 2019.

Miettinen, J. and Andersson, P.: Acoustic emission of rolling bearings lubricated with contaminated grease, Tribology

International, 33, 777–787, https://doi.org/10.1016/S0301-679X(00)00124-9, 2000.

Mirhadizadeh, S. A., Moncholi, E. P., and Mba, D.: Influence of operational variables in a hydrodynamic bearing on the

340   generation of acoustic emission, Tribology International, 43, 1760–1767, https://doi.org/10.1016/j.triboint.2010.03.003,

2010.

Mokhtari, N., Gühmann, C., and Nowoisky, S.: Approach for the Degradation of Hydrodynamic Journal Bearings based on

Acoustic Emission Feature Change: 11-13 June 2018, IEEE, Piscataway, NJ, 1 pp., 2018.

Mokhtari, N., M. Grzeszkowski, and Gühmann, C.: Vibration Signal Analysis for the Lifetime-Prediction and Failure

345   Detection of Future Turbofan Components, https://doi.org/10.24352/UB.OVGU-2017-118, 2017.

Morhain, A. and Mba, D.: Bearing defect diagnosis and acoustic emission, 653–656,

https://doi.org/10.1115/DETC2003/PTG-48083, 2003.

Morton, T. M., Harrington, R. M., and Bjeletich, J. G.: Acoustic Emissions of fatigue crack growth, 1973.

Poddar, S. and Tandon, N.: Detection of particle contamination in journal bearing using acoustic emission and vibration

350   monitoring techniques, Tribology International, 134, 154–164, https://doi.org/10.1016/j.triboint.2019.01.050, 2019.

Qu, Y., He, D., Yoon, J., van Hecke, B., Bechhoefer, E., and Zhu, J.: Gearbox tooth cut fault diagnostics using acoustic

emission and vibration sensors--a comparative study, Sensors (Basel, Switzerland), 14, 1372–1393,

https://doi.org/10.3390/s140101372, 2014.

Roberts, T. M. and Talebzadeh, M.: Fatigue life prediction based on crack propagation and acoustic emission count rates,

355   Journal of Constructional Steel Research, 59, 679–694, https://doi.org/10.1016/S0143-974X(02)00065-2, 2003.

Scheer, C., Reimche, W., and Bach, F.-W.: Early Fault Detection at Gear Units by Acoustic Emission and Wavelet Analysis,

2007.

Schnabel, S., Marklund, P., Larsson, R., and Golling, S.: The detection of plastic deformation in rolling element bearings by

acoustic emission, Tribology International, 110, 209–215, https://doi.org/10.1016/j.triboint.2017.02.021, 2017.

360 Sheng, S.: Wind turbine gearbox reliability database, condition monitoring, and O&M research update, National Laboratory

of the US Department of Energy (NREL), 2015.

Shiroishi, J., Li, Y., Liang, S., KURFESS, T., and Danyluk, S.: Bearing condition diagnostics via vibration and Acoustic

Emission measurements, Mechanical Systems and Signal Processing, 11, 693–705,

https://doi.org/10.1006/mssp.1997.0113, 1997.

365 Singh, P. J., Mukhopadhyay, C. K., Jayakumar, T., Mannan, S. L., and Raj, B.: Understanding fatigue crack propagation in

AISI 316 (N) weld using Elber's crack closure concept: Experimental results from GCMOD and acoustic emission

techniques, International Journal of Fatigue, 29, 2170–2179, https://doi.org/10.1016/j.ijfatigue.2006.12.013, 2007.

Tchakoua, P., Wamkeue, R., Ouhrouche, M., Slaoui-Hasnaoui, F., Tameghe, T., and Ekemb, G.: Wind Turbine Condition
Monitoring: State-of-the-Art Review, New Trends, and Future Challenges, Energies, 7, 2595–2630,
370   https://doi.org/10.3390/en7042595, 2014.

van Hecke, B., Yoon, J., and He, D.: Low speed bearing fault diagnosis using acoustic emission sensors, Applied Acoustics,
105, 35–44, https://doi.org/10.1016/j.apacoust.2015.10.028, 2016.

van Lier, H.: Neuhärtungsgefährdung von Radial-Zylinderrollenlagern durch Lastaufschaltungen in Betriebspunkten mit
Käfigschlupf, Zugl.: Aachen, Techn. Hochsch., Diss., 2015, Mainz, Aachen, 108 pp., 2015.

375   Venkata Rao, K. and Murthy, P. B. G. S. N.: Modeling and optimization of tool vibration and surface roughness in boring of
steel using RSM, ANN and SVM, J Intell Manuf, 29, 1533–1543, https://doi.org/10.1007/s10845-016-1197-y, 2018.

Zhang, Y., Lu, W., and Chu, F.: Planet gear fault localization for wind turbine gearbox using acoustic emission signals,
Renewable Energy, 109, 449–460, https://doi.org/10.1016/j.renene.2017.03.035, 2017.